Materials Research Bulletin 157 (2023) 112031

Contents lists available at ScienceDirect

Materials Research Bulletin

journal homepage: www.elsevier.com/locate/matresbu

Review

Nd^{3+}-doped fluoroborontellurite glass as a near-infrared optical thermometer

Renata S. Melo [a], José Carlos S. Filho [a], Nilmar S. Camilo [a], Thiago I. Rubio [b], Danilo Manzani [b,*], Acácio A. Andrade [a]

[a] Instituto de Física, Universidade Federal de Uberlândia, Uberlândia, MG 38400-902, Brazil
[b] Instituto de Química de São Carlos, Universidade de São Paulo, São Carlos, SP 13560-970, Brazil

ARTICLE INFO

Keywords:
Thermometry
Luminescence
Rare-earth ions
Relative sensitivity
Glass matrix

ABSTRACT

The determination of temperature is a very important property in many biomedical and industrial fields. In this case, the optical thermometer is an excellent alternative for conventional thermometer due it offers a fast response and can be a non-contact thermometer. In this work, a study to obtain a near-infrared optical thermometer was realized using a Nd^{3+}-doped fluoroborontellurite matrix. The study was based on the measured emission intensities of the ($^4F_{5/2}$, $^4F_{3/2}$) → $^4I_{9/2}$ transitions in the wide range of temperature from 280 up to 480 K. The changes in the emission band profiles were calibrated by means of the luminescence intensity ratio method, and the results showed that this matrix is a good candidate for an optical thermometer in the near-infrared with a relative sensitivity of 1.58% K^{-1} at room temperature. The samples with different concentrations of Nd^{3+} ions were prepared using the melt-quenching technique.

1. Introduction

The determination of temperature is a very important property in many areas such as biomedical and industrial. For biological applications it is interesting to use optical thermometry where the detection of temperature can be made by observing changes in the luminescent spectrum [1–3]. In the last few years, these optical thermometry were studied based on the luminescence of coupled levels of the rare-earth ions (RE^{3+}) such as Er^{3+} [4,5], Eu^{3+} [6,7], Pr^{3+} [8,9] and Tm^{3+} [10,11]. For example Er^{3+} has been extensively used as a primary thermometer since its luminescence intensity ratio (LIR) responds linearly to changes in temperature mainly in the physiological temperature range from 293 to 343 K.

However, many studies have focused, mainly, in the Er^{3+} and Eu^{3+} ions that have a strong emission in the visible light (green and red, respectively) [12–15]. Nevertheless, these emissions are affected by the biological tissues due to the strong scattering and absorption phenomena. To avoid that, the RE Nd^{3+} is a perfect replacer temperature sensing, since it has thermally couple levels, ^4F_j (j = 7/2, 5/2, and 3/2), and can generate far-red and near-infrared luminescence just located at the second optical window of the biological tissue [16].

The optical thermometer sensors are based on the luminescence intensity ratio (LIR) by calculating the relative emission intensity of two thermally-coupled excited states. This method allows the monitoring of only the relative changes in intensity, reducing fluctuations from other emissions, excitation source power, light scattering and other external events [17]. For the Nd^{3+} ion the LIR of the thermally coupled levels ($^4F_{3/2}$ and $^4F_{5/2}$) show remarkable change with T and thus acts as an index to probe surrounding temperature [18–20]. In this way, as Nd^{3+} ions present closely thermal-coupled energy levels, and since they are in thermal equilibrium the corresponding LIR of these states can be expressed by the Boltzmann distribution

$$LIR = I/I^* = Aexp(-\Delta E/k_BT) + y_0 \quad (1)$$

where I and I^* are the integrated intensities corresponding to the observed transitions that change with temperature. The parameters A and y_0 are adjustable constants, k_B is the Boltzmann constant, T is the absolute temperature, and ΔE is the energy difference between the excited states. Based on the expression of LIR, its value can be plotted against the absolute temperature (T) and the adjustable parameters can be obtained by the exponential fitting. As a consequence, the energy gap E is used to obtained the relative sensitivity (S_R) of temperature detection, defined by the following equations

* Corresponding author.
E-mail addresses: renatasm@ufu.br (R.S. Melo), dmanzani@usp.br (D. Manzani), acacioandrade@ufu.br (A.A. Andrade).

https://doi.org/10.1016/j.materresbull.2022.112031
Received 19 June 2022; Received in revised form 8 September 2022; Accepted 9 September 2022
Available online 14 September 2022

$$S_R = \frac{1}{LIR}\frac{d(LIR)}{dT} = \frac{\Delta E}{k_B T^2} \quad (2)$$

In this work, a set of Nd^{3+}-doped fluoroborotellurite glass was synthesized by the melt-quenching method and their thermal-optical properties were studied with the objective of application in optical thermometry in the near-infrared region. Absorption and Raman spectroscopy measurements were recorded to verify the optical and structural properties of the matrix. Experimental measurements of excited state lifetime in function of Nd^{3+} concentration were performed at room temperature under 532 nm diode laser excitation. The temperature-dependent luminescent properties of Nd^{3+}-doped glass and the luminescence intensity ratio (LIR) of the Nd^{3+}, ($^4F_{5/2}$, $^4F_{3/2}$) → $^4I_{9/2}$, emission were measured to address its probable application in optical thermometry. The results show that the material can be used as a near-infrared optical thermometer from 280 to 480 K.

2. Experimental details

A new Nd^{3+}-doped fluoroborotellurite glasses with molar composition (100-x)[60TeO_2-20BaF_2-20B_2O_3]-xNd_2O_3 (x = 0, 0.5, 1.0, 1.5, 2.0, and 3.0 mol%) were synthesized via melt-quenching method. The raw materials were stoichiometrically weighed, grounded, and mixed in an agate mortar to improve homogeneity. For each sample, the powder mixture was loaded in a gold crucible, covered with a platinum lid, and melted in an electric furnace at 750 °C for 30 min. After melting, the liquid was poured into a preheated stainless-steel mold at 280 °C and annealed for 2 h at the same temperature to remove residual stress before cooling to room temperature. Glass bulks of about 5 g were obtained and optically polished for optical characterization with final thickness about 2 mm. The characteristic temperatures such as glass transition (T_g), onset of crystallization (T_x), and maximum of crystallization (T_p) temperatures were extracted from differential scanning calorimeter (DSC) curves with an error of ± 2 °C. The T parameter was used to evaluate the thermal stability against crystallization (error of ±4 °C). DSC curves were recorded by using a DSC with DSC TA Q20 instrument from 300 to 450 °C at 10 °C.min^{-1} using aluminum-sealed crucibles under N_2 atmosphere. The absorption spectra were obtained using spectrometer Shimadzu UV3600 with a range of 340 to 1000 nm in UV–vis-NIR. The luminescence spectra were collected by using a compact spectrometer model Thorlabs CCS200 with a resolution of 4 pixels/nm, under excitation at 532 nm from 750 to 1000 nm. The resulting luminescence spectrum is the mean of multiple spectra with a standard deviation < 1 %. The excitation source was modulated by an optical chopper at a frequency of 300 Hz. The emitted light from the samples was collimated and focused in a Si photomultiplier detector. The lifetime decays present a standard deviation < 5 μs. A long-pass filter was used for luminescence and lifetime measurements, which were collected under cryogenic conditions with a cryostat Janis (model VPF-100) working from 77 K to 500 K (liquid N_2). Raman spectroscopy was performed using a LabRAM HR Evolution Horiba spectrometer in the range of 150820 cm^{-1} with a spectral resolution of 1 cm^{-1}, at 532 nm and a power of 50 mW in all measurements.

3. Results and discussion

Fig. 1 displays the absorbance spectra of the undoped and Nd^{3+}-doped fluoroborotellurite glass samples obtained as purple bulk samples in color, optically homogeneous to the unaided eye and strain-free. As it can be seen the samples are transparent from at least 400 to 1000 nm. The narrow absorption bands are assigned to the f-f electronic transitions of Nd^{3+} ground state $^4I_{9/2}$ to the excited states as labeled in Fig. 1. As expected, the absorption bands increase in intensity in function of Nd^{3+} concentration being the bands 584, 746, and 805 nm more intense as already related for silicate [21], phosphate [22], and tellurite glasses [23,24].

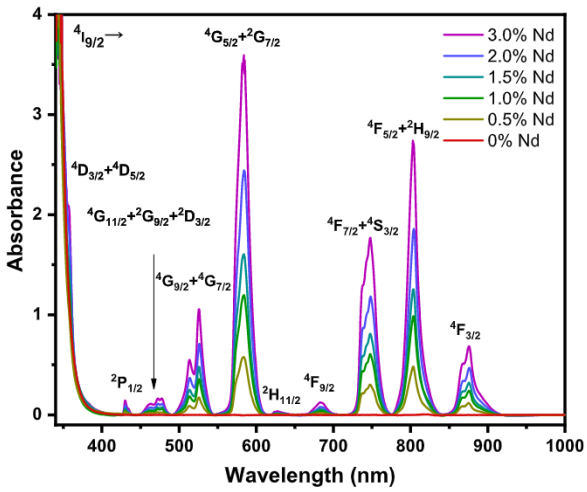

Fig. 1. Absorption spectra of Nd^{3+}-doped fluoroborontellurite glass samples.

Fig. 2 a shows the DSC curves obtained for undoped and Nd^{3+}-doped fluoroborontellurite glass samples. A homogeneous and thermal stable undoped glass was obtained with T_g and Δ T of 321 °C and > 124 °C, respectively. With Nd^{3+} doping, the T_g increases up to 1.0% doped sample (T_g = 330 °C), attributed to an increase in the network rigidity as a function of Nd_2O_3 content. On the other hand, an exothermic crystallization peak is initially observed for the 0.5% doped sample at a T_p value of 431 °C, which shifts to lower temperatures at (416 °C) for the 1.0% Nd sample. This shift is followed by a decrease in thermal stability, ΔT, suggesting that Nd^{3+} destabilizes the fluoroborontellurite network against crystallization and acts as a nucleating agent by reducing the crystallization energy in function of increased doping concentration. Despite the samples containing 1.5% and 2.0% of Nd_2O_3 presenting almost the same T_g, T_p, and ΔT of about 329 °C, 410 °C, and 62 °C, respectively, the crystallization peak also shifted to lower temperature compared to the T_p value of the 1.0% Nd sample, and even more when compared to the T_p for the 3.0% Nd sample (404 °C). The T_p shift behavior is also accompanied by a decrease of ΔT to 30 °C (3.0% Nd), reinforcing the glass modifier role of Nd_2O_3. The T_g and ΔT behaviors as a function of Nd_2O_3 content are shown in Fig. 2b.

In view of the thermal analysis results related to the decrease of thermal stability against crystallization as a function of doping concentration, Raman spectroscopy has been performed to gain an understanding of the glass network modification. In general, the Raman spectra of Nd^{3+}-doped fluoroborontellurite glass samples are dominated by the stretching modes attributed to the [TeO_n] units regardless of dopant concentration, as shown in Fig. 3. The Raman bands from 550 cm^{-1} to 1000 cm^{-1} are mainly composed by the stretching modes of three distinct polyhedral: trigonal bipyramidal units [TeO_4], [TeO_{3+1}] units resulting from [TeO_4] conversion due to the presence of BaF_2 modifier (one TeO bond is elongated), and less connected [TeO_3] units [25,26]. The band centered at 480 cm^{-1} (from 390 cm^{-1} to 550 cm^{-1}) envelops the stretching modes assigned to the symmetric inter- and intrachain of TeOTe bridge linkages and bending mode of the OTeO angle, which remains the same intensity regardless of doping concentration, attesting the low degree of glass network depolymerization promoted by the increase in Nd_2O_3 content [25,27,28]. The low-frequency bands correspond to the translatory and rotatory vibrations of the TeO_2 equatorial in a pure compound. The low-intensity Raman band centered at 290 cm^{-1} can be attributed to the bending mode of the OTeO angle because of combined vibration of the equatorial and axial oxygens atoms from [TeO_{3+1}] and [TeO_4] units [27,29].

Fig. 4 a shows the lifetime decay curves of $^4F_{3/2}$ → $^4I_{9/2}$ transition (890 nm) for the Nd^{3+}-doped glass samples. It is clearly observed a decrease of lifetime with increase of Nd^{3+} concentration from 186.9 ms

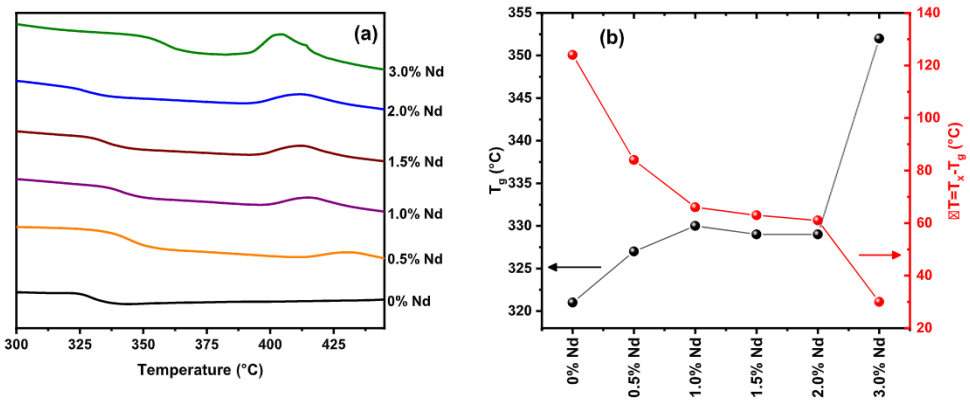

Fig. 2. (a) DSC curves obtained for Nd^{3+}-doped fluoroborontellurite glass, and (b) glass transition, T_g, and thermal stability parameter, ΔT, behavior in function of the Nd_2O_3 content in molar concentration.

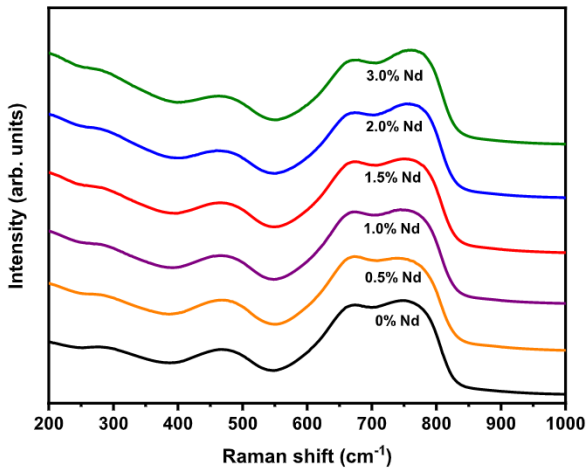

Fig. 3. Raman spectra of undoped and Nd^{3+}-doped fluoroborontellurite glass.

for 0.5% Nd sample to 48.5 ms for 3.0% Nd sample as shown in Fig. 4b. This behavior suggests a self-quenching of Nd^{3+} emission resulting from the increase of dopant concentration, which is responsible to improve non radiative decays decreasing lifetimes values through cross-relaxation (CR) effects.

In this case, the CR occurs from an excited ion $^4F_{3/2}$ that decays to $^4I_{15/2}$ level, emitting a photon and transferring part of its energy to a nearby ion in the ground state, promoting it to an excited state in which both quickly non-radiatively decay to the ground state [31] as shown in the inset of Fig. 4b. Such phenomena increase the non-radiative rate reflecting on the reduction of luminescence lifetimes [32]. This dependence is normally adjusted by the empirical equation [33]

$$\tau_{exp} = \frac{\tau_0}{1 + (N_t/Q)^p} \tag{3}$$

where τ_0 is the lifetime value observed at the limit of zero concentration, Q is the concentration where $\tau = \tau_0/2$ and p is an adjustable parameter. The data in Fig. 4b was fitted with Eq. (3), resulting in 196 μs, 1.83 mol% and 2.1, for τ_0, Q and p, respectively.

The fitted value of p being close to 2 is in good agreement with the theoretical energy transfer involving a pair of Nd^{3+} ions, with CR being the dominant non-radiative process. It is known that the experimental lifetime is defined as $\tau_{exp}^{-1} = \tau_{rad}^{-1} + W_{NR}$, where τ_{rad}^{-1} is the radiative lifetime of the ion and W_{NR} is the quenching processes of the lifetime, in this case the CR.

Fig. 5 a shows the luminescence emission spectra in the range of 775 to 950 nm under 532 nm excitation with pumping power of 50 mW. Nd^{3+}-doped sample spectra display two broad emission bands in this range assigned to $^4F_{5/2}$ and $^4F_{3/2}$ excited energy levels to the $^4I_{9/2}$ ground state at ~ 820 nm and between 840–940 nm, respectively. As can be seen, the luminescence profile of the $^4F_{3/2} \rightarrow {}^4I_{9/2}$ transition changes in function of Nd^{3+} content. As one can see, the sample 0.5% Nd has the 876 nm peak more intense than the 896 nm peak. By increasing Nd_2O_3 content, the intensity of the 876 nm peak reduces in comparison to the intensity of the 896 nm peak. This peak inversion can be attributed to the cross relaxation, where the emitted photons with energy equivalent to 11415 cm^{-1} (876 nm) can be reabsorbed by an electron in the ground-state or at the excited-state, with a fast non-radiative decay. These results indicate that decay to certain electronic transitions is prioritized

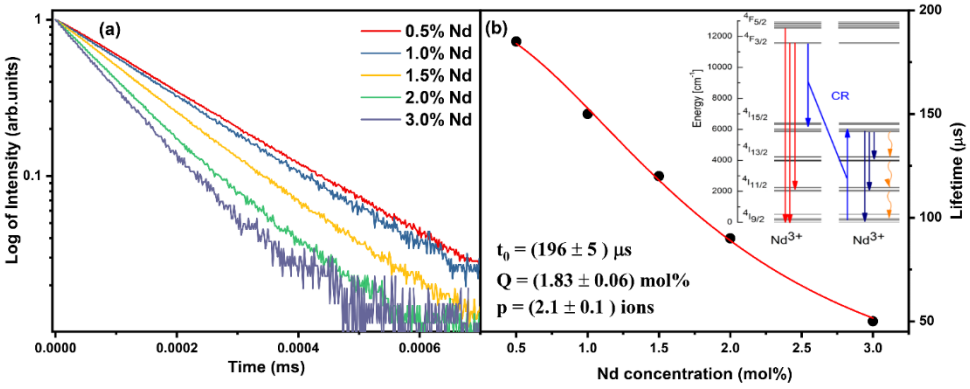

Fig. 4. (a) Log of luminescence decay curves of x% Nd^{3+} in 300K. (b) Lifetime in different samples at 300K, the inset is the energy diagram of Nd^{3+}, withdrawn and adapted from Bednarkiewicz et al. [30].

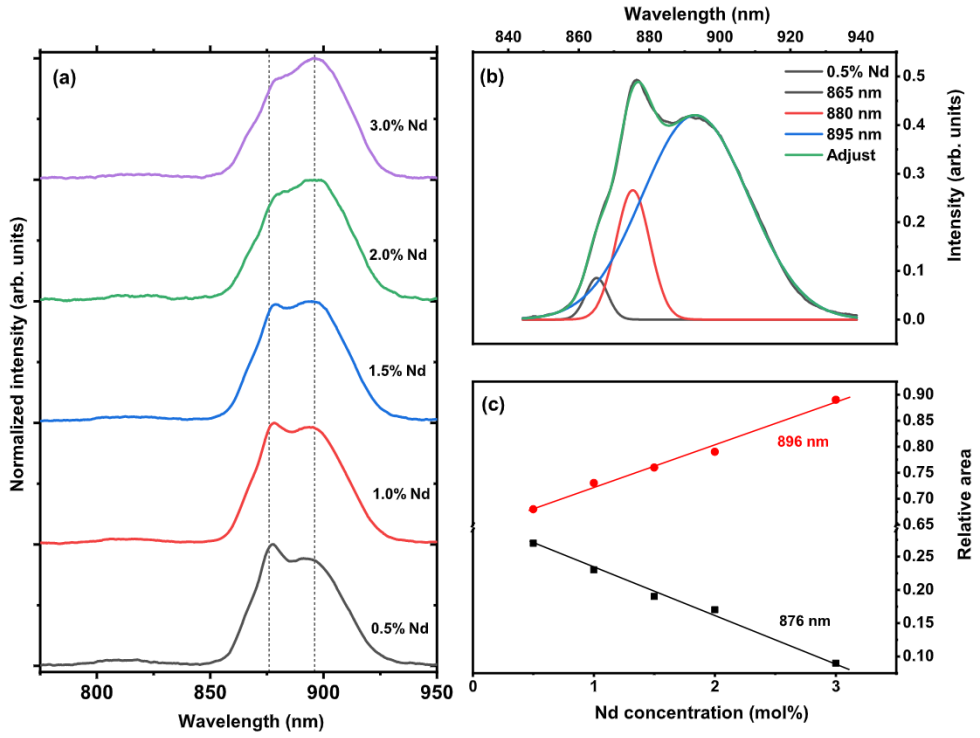

Fig. 5. (a) Luminescence spectra of Nd^{3+}-doped fluoroborontellurite samples at room temperature. The dashed lines mark the wavelength at 876 and 896 nm. (b) luminescence deconvoluted band of 0.5% Nd sample (c) luminescence area of 876 nm and 896 nm deconvoluted bands in respect to Nd_2O_3 content.

with the increase concentration. Fig. 5b shows the deconvolution of the 0.5% Nd sample in 3 bands at 865, 876, and 896 nm, which correspond to the Stark levels of the metastable $^4F_{3/2}$ levels. Fig. 5c shows the luminescence area of 876 nm and 896 nm deconvoluted bands in respect to Nd_2O_3 content. From our best knowledge, this change in the profile of the $^4F_{3/2} \rightarrow {}^4I_{9/2}$ transition was not observed before in function of doping concentration.

In order to verify if this system is a candidate for an optical thermometer, we also have made the luminescence measurement in function of temperature. Fig. 6a shows the luminescence spectra 0.5% Nd sample

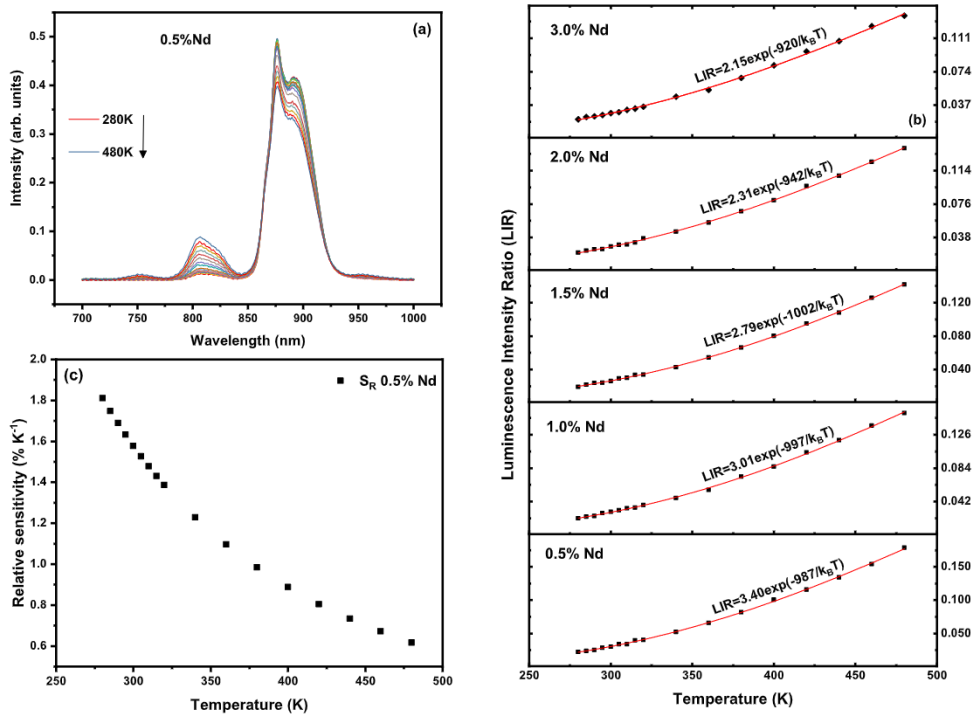

Fig. 6. (a) Luminescence spectra of 0.5% Nd^{3+} as a function of temperature, and (b) luminescence intensity ratio of the bands at 820 and 890 nm for x% Nd^{3+}, where the red line is the Boltzmann distribution fit (c) relative sensitivity of 0.5% Nd^{3+} for 280–480 K. (For interpretation of the references to colour in this figure legend, the reader is referred to the web version of this article.)

in function of temperature from 280 to 480 K, in which the area of $^4F_{5/2} \rightarrow {}^4I_{9/2}$ and $^4F_{3/2} \rightarrow {}^4I_{9/2}$ thermal coupled levels, assigned to the bands centered at 820 nm and 890 nm, respectively, change with the temperature. As can be seen, the band area centered at 820 nm increases with temperature while the band area centered at 890 nm decreases. The luminescence intensity ratio (LIR) of these bands was made for all samples as presented in Fig. 6b. The data were fitted by Boltzmann distribution (Eq. (1)) as shown by the red solid line. From the fit was found the adjustable parameter E and that correspond the energy difference between the excited states $^4F_{3/2}$ and $^4F_{5/2}$ and the values were (987 ± 30) cm^{-1}, (997 ± 30) cm^{-1}, (1002 ± 30) cm^{-1}, (942 ± 30) cm^{-1} and (920 ± 30) cm^{-1} to sample with 0.5%, 1.0%, 1.5%, 2.0% and 3.0% of Nd^{3+} respectively. The relative sensitivity in function of the temperature can be obtained by using the value of E in the Eq. (2). As the sample with 0.5% Nd^{3+} has the higher LIR variation in the studied range of temperature, this sample has the best relative sensitivity and the found values are shown in Fig. 6c. The uncertainty in temperature was obtained using the equation $\delta T = 1/S_R \delta LIR/LIR$, which varies between 0.6 and 1.8 K in the range of temperature 280-480K, where $\delta LIR/LIR$ is about 1%, obtained from the standard deviation of multiple luminescence spectra. Comparing the results with other works from literature, as shown in Table 1, we can see that our S_R value at 300 K is in the same order of magnitude.

In addition, in order to verify if the studied optical thermometer is a primary thermometer, *i.e.* if this thermometer can be used without a reference, it was calculated the temperature for the LIR values of the 0.5% Nd^{3+} sample (Fig. 6b) using the equation $T = [1/T_0 - (k_B/\Delta E)\ ln(LIR/LIR_0)]^{-1}$ [41], as shown in Fig. 7 (blue solid circle), where T_0 is the room temperature, LIR_0 is the LIR value at room temperature and $\Delta E = 987$ cm^{-1}. By adjusting the data with a linear expression, the angular coefficient obtained was 0.995, and the correlation coefficient R = 0.999. As observed, the linear adjustment (red line) of calculated temperature (blue solid circles) matches with the expected temperatures (black line), indicating that this studied optical thermometer is a primary optical thermometer.

Table 1
Relative sensibility for Nd^{3+} ions in glass and ceramic media.

Optical thermometric materials	T (K)	$S_{Rmax}(\%K^{-1})$	Refs.
$LaSrGaO_4$	300	0.19	[34]
Y_2SiO_5	300	1.44	[35]
$P_2O_5 - Al_2O_3 - Na_2O - K_2O$	300	1.5	[36]
$TeO_2 - BaF_2 - B_2O_3 : Nd_2O_3$	300	1.58	This work
$Ba_4La_2Ti_4Nb_6O_30$	300	1.83	[37]
$LaPO_4$	280	1.72	[38]
Y_2O_3	290	1.51	[39]
$NaYF^4 : Yb^{3+}/Nd^{3+}$	416	1.05	[18]
$SiO_2 - AlF_3 - BaF_2 - LaF_3 : EuF_3$ /NdF	420	1.02	[20]
$Sr_{1-x}BaxNb_2O_6 : Nd^{3+}$	600	0.17	[40]

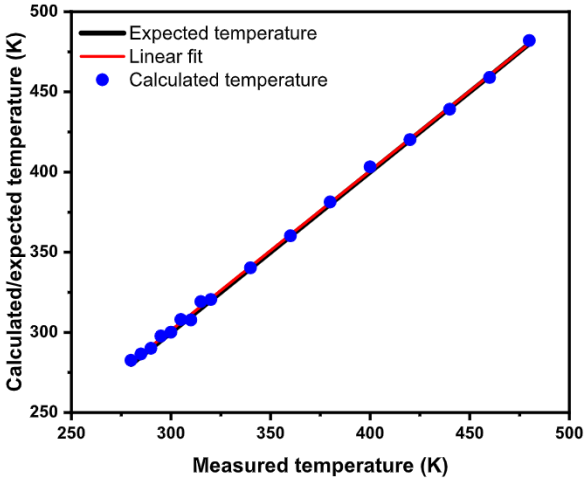

Fig. 7. The black line is the expected temperature, the blue solid circles are the calculated temperature and the red line is the linear fit of the 0.5% Nd^{3+} sample experimental data. (For interpretation of the references to colour in this figure legend, the reader is referred to the web version of this article.)

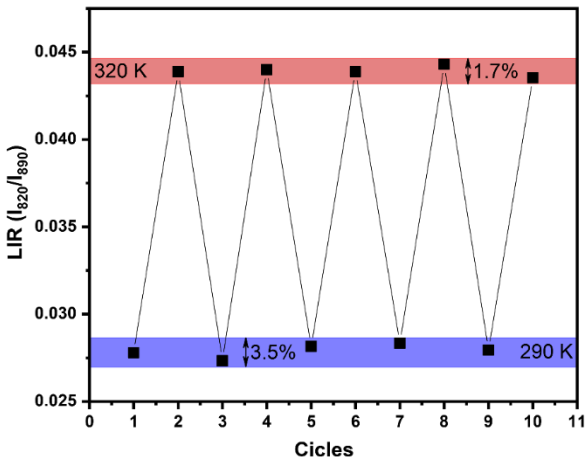

Fig. 8. Repeatability of 0.5% Nd^{3+} sample for temperature cycling of LIR. The spectra were collected in heating (320 K) and cooling (290 K) cycles.

Finally, the repeatability of the thermometric correlation was obtained from the integrated intensity ratio between the $^4F_{3/2} \rightarrow {}^4I_{9/2}$ (I_{820}) and $^4F_{5/2} \rightarrow {}^4I_{9/2}$ (I_{890}) Nd^{3+} for the sample of 0.5% Nd^{3+}. The spectra were collected in heating (320 K) and cooling (290 K) cycles. As can be seen in Fig. 8, in 290 K the variation of LIR was only 3.5%, which corresponds to a maximum temperature variation of $\delta T_{max} = 2.2$ K. Moreover, according to Fig. 8, this variation decreases for highest temperatures increasing its accuracy and precision.

4. Conclusions

In this work, we demonstrate the application of a Nd^{3+}-doped fluoroborontellurite glass as a near-infrared optical thermometer from 280 to 480 K through luminescence intensity ratio of two thermal coupled transitions. The Nd^{3+} concentration was varied and it did not significantly modify the glass network, as shown by Raman spectroscopy, was observed. From luminescence spectra at room temperature, it was observed that the profile of the emission bands related to the $^4F_{3/2} \rightarrow {}^4I_{9/2}$ and $^4F_{5/2} \rightarrow {}^4I_{9/2}$ transitions changes with the addition of Nd_2O_3. Moreover, the results of measurements of luminescence decay showed an increase in the cross relaxation with the increase of Nd^{3+} doping, and such a process can distort the emission spectrum with a quenching in the intensity at 876 nm peak. Finally, luminescence measurements in function of temperature, also show an opposite behavior of emission intensity of bands centered 820 nm (increase intensity) and 890 nm (decrease in intensity) showing a thermal dependence between them to populate these levels. In general, the overall results demonstrated that stable Nd^{3+}-doped fluoroborontellurite glass can be obtained and is suitable for application as primary optical thermometer operating in the infrared region with a relative sensitivity of 1.58% K^{-1} at 300 K, value comparable to those found in the literature.

Declaration of Competing Interest

The authors declare that they have no known competing financial interests or personal relationships that could have appeared to influence the work reported in this paper.

Data availability

The data that has been used is confidential.

Acknowledgments

The authors are grateful to the Brazilian National Research Council (CNPq), CAPES-Finance Code 001, FAPEMIG, FAPESP (2019/16230-1 and 2018/14261-4) and INCT/Institute of Photonics (INFO) for the financial support.

References

[1] G. Xiang, Q. Xia, X. Liu, Y. Wang, S. Jiang, L. Li, X. Zhou, L. Ma, X. Wang, J. Zhang, Upconversion nanoparticles modified by Cu 2 S for photothermal therapy along with real-time optical thermometry, Nanoscale 13 (15) (2021) 7161–7168.
[2] G. Xiang, M. Yang, Z. Liu, Y. Wang, S. Jiang, X. Zhou, L. Li, L. Ma, X. Wang, J. Zhang, Near-infrared-to-near-infrared optical thermometer Bay2O4: Yb3+/Nd3+ assembled with photothermal conversion performance, Inorg. Chem. 61 (13) (2022) 5425–5432.
[3] D.T. Vu, Y.-C. Tsai, Q.M. Le, S.-W. Kuo, N.D. Lai, H. Benisty, J.-Y. Lin, H.-C. Kan, C.-C. Hsu, A synergy approach to enhance upconversion luminescence emission of rare earth nanophosphors with million-fold enhancement factor, Crystals 11 (10) (2021) 1187.
[4] D. Manzani, J.a.F.d.S. Petruci, K. Nigoghossian, A.A. Cardoso, S.J.L. Ribeiro, A portable luminescent thermometer based on green up-conversion emission of Er3+/Yb3+ co-doped tellurite glass, Sci. Rep. 7 (1) (2017) 1–11.
[5] Y. Wu, H. Suo, D. He, C. Guo, Highly sensitive up-conversion optical thermometry based on Yb3+-Er3+ co-doped NaLa (MoO4) 2 green phosphors, Mater. Res. Bull. 106 (2018) 14–18.
[6] R.G. Geitenbeek, H.W. De Wijn, A. Meijerink, Non-Boltzmann luminescence in Na Y F 4: Eu 3+: implications for luminescence thermometry, Phys. Rev. Appl. 10 (6) (2018) 064006.
[7] Y. Ding, N. Guo, M. Zhu, W. Lv, R. Ouyang, Y. Miao, B. Shao, Luminescence and temperature sensing abilities of zincate phosphors co-doped bismuth Bi3+ and lanthanide Eu3+/Sm3+, Mater. Res. Bull. 129 (2020) 110869.
[8] H. Zhang, Z. Gao, G. Li, Y. Zhu, S. Liu, K. Li, Y. Liang, A ratiometric optical thermometer with multi-color emission and high sensitivity based on double perovskite LaMg0.402Nb0.598O3: Pr3+ thermochromic phosphors, Chem. Eng. J. 380 (2020) 122491.
[9] E. Zhao, X. Liu, D. Tang, L. Liu, G. Liu, B. Zhou, C. Xing, 800 nm laser induced white light upconversion of Nd/Yb/Pr triply doped NaYF4 through a dual-sensitization strategy, Mater. Res. Bull. 133 (2021) 111027.
[10] W. Chen, F. Hu, R. Wei, Q. Zeng, L. Chen, H. Guo, Optical thermometry based on up-conversion luminescence of Tm3+ doped transparent Sr2YF7 glass ceramics, J. Lumin. 192 (2017) 303–309.
[11] X. Tu, J. Xu, M. Li, T. Xie, R. Lei, H. Wang, S. Xu, Color-tunable upconversion luminescence and temperature sensing behavior of Tm3+/Yb3+ codoped Y2Ti2O7 phosphors, Mater. Res. Bull. 112 (2019) 77–83.
[12] M. Suta, A. Meijerink, A theoretical framework for ratiometric single ion luminescent thermometers–thermodynamic and kinetic guidelines for optimized performance, Adv. Theory Simul. 3 (12) (2020) 2000176.
[13] V. Lojpur, S. Ćulubrk, M. Medić, M. Dramicanin, Luminescence thermometry with Eu3+ doped GdAlO3, J. Lumin. 170 (2016) 467–471.
[14] I.E. Kolesnikov, A.A. Kalinichev, M.A. Kurochkin, D.V. Mamonova, E. Y. Kolesnikov, E. Lahderanta, Ratiometric optical thermometry based on emission and excitation spectra of YVO4: Eu3+ nanophosphors, J. Phys. Chem. C 123 (8) (2019) 5136–5143.
[15] I.E. Kolesnikov, D.V. Mamonova, M.A. Kurochkin, E.Y. Kolesnikov, E. Lahderanta, Optical thermometry by monitoring dual emissions from YVO4 and Eu3+ in YVO4: Eu3+ nanoparticles, ACS Appl. Nano Mater. 4 (2) (2021) 1959–1966.
[16] I.E. Kolesnikov, A.A. Kalinichev, M.A. Kurochkin, E.V. Golyeva, E.Y. Kolesnikov, A. V. Kurochkin, E. Lähderanta, M.D. Mikhailov, YVO4: Nd3+ nanophosphors as NIR-to-NIR thermal sensors in wide temperature range, Sci. Rep. 7 (1) (2017) 1–8.
[17] C.D.S. Brites, P.P. Lima, N.J.O. Silva, A. Millán, V.S. Amaral, F. Palacio, L.D. Carlos, Thermometry at the nanoscale, Nanoscale 4 (16) (2012) 4799–4829.
[18] Z. Cai, S. Kang, X. Huang, X. Song, X. Xiao, J. Qiu, G. Dong, A novel wide temperature range and multi-mode optical thermometer based on bi-functional nanocrystal-doped glass ceramics, J. Mater. Chem. C 6 (37) (2018) 9932–9940.
[19] W.J. Faria, T.S. Gonçalves, A.S.S. de Camargo, Near infrared optical thermometry in fluorophosphate glasses doped with Nd3+ and Nd3+/Yb3+, J. Alloy. Compd. 883 (2021) 160849.
[20] Z. Zhao, F. Hu, Z. Cao, F. Chi, X. Wei, Y. Chen, C.K. Duan, M. Yin, Self-crystallized Ba2LaF7:Nd3+/Eu3+ glass ceramics for optical thermometry, Ceram. Int. 43 (17) (2017) 14951–14955.
[21] E.O. Serqueira, N.O. Dantas, V. Anjos, M.A. Pereira-da Silva, M. Bell, Optical spectroscopy of Nd3+ ions in a nanostructured glass matrix, J. Lumin. 131 (7) (2011) 1401–1406.
[22] N.O. Dantas, E.O. Serqueira, A.C.A. Silva, A.A. Andrade, S.A. Lourenço, High quantum efficiency of Nd3+ ions in a phosphate glass system using the Judd–Ofelt theory, Braz. J. Phys. 43 (4) (2013) 230–238.
[23] K. Linganna, R. Narro-García, H. Desirena, E. De la Rosa, C. Basavapoornima, V. Venkatramu, C.K. Jayasankar, Effect of P2O5 addition on structural and luminescence properties of Nd3+-doped tellurite glasses, J. Alloys Compd. 684 (2016) 322–327.
[24] Z. Zhou, Y. Zhou, M. Zhou, X. Su, P. Cheng, The enhanced near-infrared fluorescence of Nd3+-doped tellurite glass, J. Non Cryst. Solids 470 (2017) 122–131.
[25] J.M.M. de Souza, K. de Oliveira Lima, J.L. Ferrari, L.J.Q. Maia, R.R. Gonçalves, R. F. Falci, D. Manzani, Photoluminescence properties of Er3+ and Er3+/Yb3+ doped tellurite glass and glass-ceramics containing Bi2Te4O11 crystals, Dalton Trans. 51 (10) (2022) 4087–4096.
[26] D. Manzani, J.B.S. Junior, A.S. Reyna, M.L.S. Neto, J.E.Q. Bautista, S.J.L. Ribeiro, C.B. De Araújo, Phosphotellurite glass and glass-ceramics with high TeO2 contents: thermal, structural and optical properties, Dalton Trans. 48 (18) (2019) 6261–6272.
[27] E.A. Lalla, A. Sanz-Arranz, M. Konstantinidis, J. Freemantle, P. Such, A.D. Lozano-Gorrín, V. Lavin, G. Lopez-Reyes, F. Rull-Pérez, U.R. Rodríguez-Mendoza, Raman-IR spectroscopic structural analysis of rare-earth (RE3+) doped fluorotellurite glasses at different laser wavelengths, Vib. Spectrosc. 106 (2020) 103020.
[28] M. Ceriotti, F. Pietrucci, M. Bernasconi, Ab initio study of the vibrational properties of crystalline TeO2: the α, β, and γ phases, Phys. Rev. B 73 (10) (2006) 104304.
[29] V. Rodriguez, M. Couzi, F. Adamietz, M. Dussauze, G. Guery, T. Cardinal, P. Veber, K. Richardson, P. Thomas, Hyper-raman and raman scattering in paratellurite TeO2, J. Raman Spectrosc. 44 (5) (2013) 739–745.
[30] A. Bednarkiewicz, D. Wawrzynczyk, M. Nyk, W. Strek, Optically stimulated heating using Nd3+ doped NaYF4 colloidal near infrared nanophosphors, Appl. Phys. B 103 (4) (2011) 847–852.
[31] A.A. Andrade, S.M. Lima, V. Pilla, J.A. Sampaio, T. Catunda, M.L. Baesso, Fluorescence quantum efficiency measurements using the thermal lens technique, Rev. Sci. Instrum. 74 (1) (2003) 857–859.
[32] R. Jacobs, M. Weber, Dependence of the 4 F 3/2 → 4 I 11/2 induced-emission cross section for Nd3+ on glass composition, IEEE J Quantum Electron 12 (2) (1976) 102–111.
[33] W.J. Miniscalco, Optical and electronic properties of rare earth ions in glasses, Opt. Eng. 71 (2001) 17–112.
[34] Z. Xing, P. Li, S. Wu, C. Liu, D. Dai, X. Li, L. Zhang, D. Wang, Z. Yang, Z. Wang, A perovskite-like LaSrGaO44: Mn2+, Nd3+, Yb3+ NIR luminescent material for fluorescent temperature sensor, J. Lumin. 225 (2020) 117352.
[35] G.S. Maciel, N. Rakov, Thermometric analysis of the near-infrared emission of Nd3+ in Y2SiO5 ceramic powder prepared by combustion synthesis, Ceram. Int. 46 (8) (2020) 12165–12171.
[36] D.N. Messias, V. Pilla, A.C. Silva, N.O. Dantas, A.A. Andrade, et al., Temperature-dependence on the lifetime of Nd3+-doped phosphate glass, J. Lumin. 219 (2020) 116901.
[37] Y. Shi, F. Yang, C. Zhao, Y. Huang, M. Li, Q. Zhou, Q. Li, Z. Li, J. Liu, T. Wei, Highly sensitive up-conversion thermometric performance in Nd3+ and Yb3+ sensitized Ba4La2Ti4Nb6O30 based on near-infrared emissions, J. Phys. Chem. Solids 124 (2019) 130–136.
[38] H. Suo, X. Zhao, Z. Zhang, C. Guo, Ultra-sensitive optical nano-thermometer LaPO4: Yb3+/Nd3+ based on thermo-enhanced NIR-to-NIR emissions, Chem. Eng. J. 389 (2020) 124506.
[39] I.E. Kolesnikov, A.A. Kalinichev, M.A. Kurochkin, D.V. Mamonova, E. Y. Kolesnikov, E. Lähderanta, M.D. Mikhailov, Bifunctional heater-thermometer Nd3+-doped nanoparticles with multiple temperature sensing parameters, Nanotechnology 30 (14) (2019) 145501.
[40] P. Haro-González, I.R. Martín, L.L. Martín, S.F. León-Luis, C. Pérez-Rodríguez, V. Lavín, Characterization of Er3+ and Nd3+ doped strontium barium niobate glass ceramic as temperature sensors, Opt. Mater. 33 (5) (2011) 742–745.
[41] C.D.S. Brites, S. Balabhadra, L.D. Carlos, Lanthanide-based thermometers: at the cutting-edge of luminescence thermometry, Adv. Opt. Mater. 7 (5) (2019) 1801239.